

---

# Noise Estimation Is Not Optimal: How to Use Kalman Filter the Right Way

---

**Ido Greenberg**

Department of Electric Engineering,  
Technion, Israel  
gido@campus.technion.ac.il

**Netanel Yannay**

**Shie Mannor**  
Department of Electric Engineering,  
Technion, Israel  
Nvidia Research

## Abstract

Determining the noise parameters of a Kalman Filter (KF) has been studied for decades. A huge body of research focuses on the task of estimation of the noise under various conditions, since precise noise estimation is considered equivalent to minimization of the filtering errors. However, we show that even a small violation of the KF assumptions can significantly modify the *effective* noise, breaking the equivalence between the tasks and making noise estimation an inferior strategy. We show that such violations are very common, and are often not trivial to handle or even notice. Consequentially, we argue that a robust solution is needed – rather than choosing a dedicated model per problem. To that end, we apply gradient-based optimization to the filtering errors directly, with relation to a simple and efficient parameterization of the symmetric and positive-definite parameters of KF. In radar tracking and video tracking, we show that the optimization improves both the accuracy of KF and its robustness to design decisions. In addition, we demonstrate how an optimized neural network model can seem to reduce the errors significantly compared to a KF – and how this reduction vanishes once the KF is optimized similarly. This indicates how complicated models can be wrongly identified as superior to KF, while in fact they were merely more optimized.

## 1 Introduction

The Kalman Filter (KF) [Kalman, 1960] is a celebrated method for linear filtering and prediction, with applications in many fields including tracking, guidance, navigation and control [Zarchan and Musoff, 2000, Kirubarajan, 2002]. Due to its simplicity and robustness, it remains highly popular – with over 10,000 citations in the last 5 years alone [Google Scholar, 2021] – despite the rise of many non-linear sequential prediction models (e.g., recurrent neural networks). The KF relies on the following model for a dynamic system:

$$\begin{aligned} X_{t+1} &= FX_t + \omega_t & (\omega_t &\sim N(0, Q)) \\ Z_t &= HX_t + \nu_t & (\nu_t &\sim N(0, R)) \end{aligned} \quad (1)$$

where  $X_t$  is the (unknown) state of the system at time  $t$ , whose dynamics are modeled by the linear operator  $F$  up to the random noise  $\omega_t$  with covariance  $Q$ ; and  $Z_t$  is the observation, which is modeled by the linear operator  $H$  up to the noise  $\nu_t$  with covariance  $R$ .

Many works have addressed the challenge of determining the noise parameters  $Q, R$  [Abbeel et al., 2005, Odelson et al., 2006, Zanni et al., 2017, Park et al., 2019]. Since the KF yields minimal errors when  $Q$  and  $R$  correspond to the true covariance matrices of the noise [Humpherys et al., 2012], these parameters are usually determined by noise estimation. This is particularly true when the training data contain the ground-truth (i.e., the system states), in which case the noise can be trivially estimated by the sample covariance matrix. Other methods are needed in absence of the ground-truth, but as stated

by Odelson et al. [2006], “*the more systematic and preferable approach to determine the filter gain is to estimate the covariances from data*”. This work focuses on such problems with ground-truth available for learning (but not for inference after the learning, of course), which was motivated by a real-world Doppler radar estimation problem.

**Noise estimation is not optimal:** The equivalence between noise estimation and errors minimization can be proved under the standard assumptions of KF – that is, known and linear dynamics and observation models  $(F, H)$ , with i.i.d and normally-distributed noises  $(\{\omega_t\}, \{\nu_t\})$  [Humpherys et al., 2012]. However, as put by Thomson [1994], “*experience with real-world data soon convinces one that stationarity and Gaussianity are fairy tales invented for the amusement of undergraduates*” – and linearity and independence can be safely added to this list. Therefore, under realistic assumptions, the covariance of the noise does not necessarily correspond to optimal filtering.

We introduce a case study in the context of radar tracking, where we demonstrate that even using the exact covariance of the noise (“oracle-based” parameters) is highly sub-optimal – even in very simplistic scenarios with relatively minor violation of KF assumptions. We analyze this phenomenon analytically for the case of non-linear observation model in a Doppler radar, where the violation of linearity is shown to modify the effective noise. By providing this extensive evidence for the sub-optimality of noise estimation in practical applications of the KF, **we re-open a problem that was considered solved for decades** [Kalman, 1960].

We also show that seemingly small changes in the properties of the scenario sometimes lead to major changes in the desired design of the KF, e.g., whether to use a KF or an Extended KF [Julier and Uhlmann, 2004]. In certain cases, the design choices are easy to overlook (e.g., Cartesian vs. polar coordinates), and are not trivial to make even if noticed. As a result, it is impractical to manually choose or develop a variant of KF for every problem. Rather, we should assume that our model is sub-optimal, and leverage data to deal with the sub-optimality as robustly as possible.

**How to use KF the right way:** We consider  $Q$  and  $R$  as model parameters that should be optimized with respect to the filtering errors – rather than estimating the noise. While both noise estimation and errors optimization rely on exploitation of data, only the latter explicitly addresses the actual goal of solving the filtering problem.

Many gradient-based optimization methods have been demonstrated effective in the field of machine learning, but applying them naively to the entries of  $Q$  and  $R$  may violate the symmetry and positive-definiteness (SPD) constraints of the covariance matrices. Indeed, even works that come as far as optimizing  $Q$  and  $R$  (instead of estimating the noise) usually apply limited optimization methods, e.g., grid-search [Coskun et al., 2017] or diagonal restriction of the covariance matrices [Formentin and Bittanti, 2014, Li et al., 2019]. To address this issue, we use a parameterization based on Cholesky decomposition [Horn and Johnson, 1985], which allows us to apply gradient-based optimization to SPD matrices. This method is computationally efficient compared to other general gradient-based methods for SPD optimization [Tsuda et al., 2005, Tibshirani, 2015].

We demonstrate that the optimization reduces the errors of KF consistently: over different variants of KF, over different scenarios of radar tracking, and even in the different domain of tracking from video. In most cases, the likelihood score of the tracker is improved as well, which is important for matching of observations to targets in the multi-target tracking problem. Furthermore, we show that optimization improves the robustness to design decisions, by shrinking the gaps between the performance of different variants of KF. We also demonstrate that optimization generalizes well under distributional shifts between train and test data, and in that sense does not overfit the train data more than noise estimation.

As explained above, we *extensively* justify the need to optimize KF in almost any practical problem, and suggest a simple solution that is effective, robust, computationally efficient, and relies on standard tools in supervised machine learning. As a result, we believe that in the scope of filtering problems with available ground-truth, **the suggested optimization method is capable of becoming the new standard procedure for tuning of KF**.

**Unfair comparison:** Many learning algorithms have been suggested to address non-linearity in filtering problems, e.g., based on Recurrent Neural Networks (RNN). Such works often use a linear tool such as the KF as a baseline for comparison – with tuning parameters being sometimes ignored

[Gao et al., 2019], sometimes based on noise estimation [fa Dai et al., 2020], and sometimes optimized in a limited manner using trial-and-error [Jamil et al., 2020] or grid-search [Coskun et al., 2017]. Our findings imply that such a methodology yields over-optimistic conclusions, since the baseline is not optimized to the same level as the learning model. This may result in adoption of over-complicated algorithms with no actual added value. Instead, any learning algorithm should be compared to a baseline that is optimized using a similar method (e.g., gradient-descent with respect to the errors).

Indeed, we consider an extension of KF based on LSTM, which is the key component in most SOTA algorithms for non-linear sequential prediction in recent years [Neu et al., 2021]. For radar tracking with non-linear motion, we demonstrate how the LSTM seems to provide a significant improvement over the KF. Then, we show that the whole improvement comes from optimization of parameters, and *not* from the expressive non-linear architecture. In particular, this result demonstrates the competitiveness of our suggested method versus SOTA sequential prediction models.

Recent works in the area of machine learning have already shown that advanced algorithms often obtain most of their improvement from implementation nuances [Engstrom et al., 2019, Andrychowicz et al., 2020, Henderson et al., 2017]. Our work continues this line of thinking and raises awareness to this issue in the domain of filtering problems, in order to enhance the value of existing algorithms, and avoid unnecessarily complicated and costly ones.

**Contribution:** We show that KF is used incorrectly in a variety of problems; show that advanced filtering algorithms are often tested unfairly; suggest a simple method to solve both issues, using gradient-based optimization along with Cholesky decomposition; and provide a detailed case study that analyzes the differences between noise estimation and parameters optimization empirically and (for a specific benchmark) analytically.

The paper is organized as follows: Section 2 reviews KF and RNN. Section 3 demonstrates the necessity of optimization in KF through a detailed case study. Section 4 introduces our method for efficient optimization of KF parameters. Section 5 presents a neural version of KF which reduces the errors compared to a standard KF – but not when compared to an optimized KF. Section 6 discusses related works, and Section 7 summarizes.

## 2 Preliminaries and Problem Setup

**Kalman Filter:** The KF algorithm relies on the model of Eq. (1) for a dynamic system. It keeps an estimate of the state  $X_t$ , represented as the mean  $x_t$  and covariance  $P_t$  of a normal distribution. As shown in Figure 1, it alternately predicts the next state using the dynamics model (*prediction* step), and processes new information from incoming observations (*update* or *filtering* step).

While being useful and robust, KF yields optimal estimations only under a restrictive set of assumptions [Kalman, 1960], as specified in Definition 2.1.

**Definition 2.1** (KF assumptions).  $F, H$  of Eq. (1) are constant and known matrices;  $\omega_t, \nu_t$  are i.i.d random variables with zero-mean and constant, known covariance matrices  $Q, R$ , respectively; and the distribution of the random initial state  $X_0$  is known.

Note that both motion and observation models in Definition 2.1 are assumed to be linear, and both sources of noise are i.i.d with known covariance. Normality of the noise is also often assumed, but is not necessary for optimality [Humpherys et al., 2012].

Violations of some of the assumptions in Definition 2.1 can be handled by certain variations of the KF, such as the Extended KF (EKF) [Julier and Uhlmann, 2004] which replaces the linear models  $F, H$  with local linear approximations, and the Unscented KF (UKF) [Wan and Van Der Merwe,

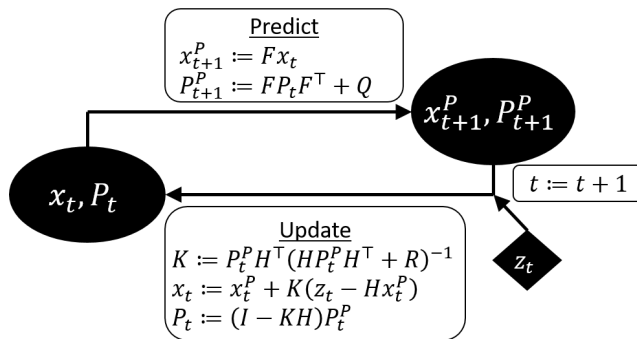


Figure 1: A diagram of the KF algorithm. Note that the prediction step is based on the motion model  $F$  with noise  $Q$ , whereas the update step is based on the observation model  $H$  with noise  $R$ .

2000] which applies particle-filtering approach. The use of multiple tracking models alternately is also possible using switching mechanisms [Mazor et al., 1998].

While  $F$  and  $H$  are usually determined based on domain knowledge,  $Q$  and  $R$  are often estimated from data as the covariance of the noise. Many works consider the problem of estimation from the observations alone, but when the true states are available in the data, the estimation becomes a straight-forward computation of the sample covariance matrices [Lacey, 1998]:

$$\hat{R} := Cov(\{z_t - Hx_t\}_t), \quad \hat{Q} := Cov(\{x_{t+1} - Fx_t\}_t). \quad (2)$$

**Recurrent neural networks:** A RNN [Rumelhart et al., 1986] is a neural network that is intended to be iteratively fed with sequential data samples, and that passes information (the *hidden state*) over iterations. Every iteration, the hidden state is fed to the next copy of the network as part of its input, along with the new data sample. *Long Short Term Memory* (LSTM) [Hochreiter and Schmidhuber, 1997] is an architecture of RNN that is particularly popular due to the linear flow of the hidden state over iterations, allowing it to capture memory for relatively long term. The parameters of a RNN are usually optimized in a supervised manner with respect to a training dataset of input-output pairs.

For a more detailed introduction of the preliminaries, see Appendix A.

### 3 Kalman Filter Configuration and Optimization: a Case Study

In this section, we compare noise estimation and errors optimization in KF through a detailed case study. Once we understand the importance of optimization in KF, Section 4 discusses its challenges and suggests an efficient optimization method under the constraints of KF.

The performance of a KF strongly depends on its parameters  $Q$  and  $R$ . These parameters are usually regarded as estimators of the noise covariance in motion and observation, respectively [Lacey, 1998], and are estimated accordingly. Even though optimization has been suggested for KF in the past [Abbeel et al., 2005], it was often viewed as a fallback solution [Odelson et al., 2006], for cases where direct estimation is not possible (e.g., the true states are unavailable in the data [Feng et al., 2014]), or where the problem is more complicated (e.g., non-stationary noise [Akhlaghi et al., 2017]).

The preference of estimation relies on the fact that KF – with parameters corresponding to the noise covariances – provides optimal filtering errors. However, the optimality only holds under the assumptions specified in Definition 2.1 [Humpherys et al., 2012]. Some of these assumptions are clearly violated in realistic scenarios, while other violations may be less obvious. For example, even if a radar’s noise is i.i.d in polar coordinates, it is not so in Cartesian coordinates (see Appendix A.4).

The need to rely on many assumptions might explain why there are several extensions and design decisions in the configuration of a KF. This includes the choice between KF and EKF [Julier and Uhlmann, 2004]; the choice between educated state initialization and a simple uniform prior [Linderoth et al., 2011]; and certain choices that may be made without even noticing, such as the coordinates of the state representation.

The case study below justifies the following claims:

1. The design decisions in KF are often nontrivial to make and are potentially significant.
2. Tuning KF by noise estimation is often highly sub-optimal – even in very simple scenarios.
3. Tuning KF by optimization improves both accuracy and robustness to design decisions.

These claims mean that the popular KF algorithm is often not exploited to its full potential. Furthermore, many works that compare learning algorithms to a KF baseline conduct an "unfair" comparison, as the learning algorithms are optimized and the KF is not. This may lead to adoption of unnecessarily complicated algorithms, as demonstrated in Section 5. Indeed, in many works the tuning of the baseline KF is either ignored in the report [Gao et al., 2019] or relies on noise estimation [fa Dai et al., 2020], sometimes directly by the observing sensor [Jamil et al., 2020].

#### 3.1 Setup and methodology

In the case study of the radar tracking problem, each target is represented by a sequence of (unknown) states in consecutive time-steps, and a corresponding sequence of radar measurements. A state

$x_{full} = (x_x, x_y, x_z, x_{vx}, x_{vy}, x_{vz})^\top \in \mathbb{R}^6$  consists of 3D location and velocity. We also denote  $x = (x_x, x_y, x_z)^\top \in \mathbb{R}^3$  for the location alone (or  $x_{target,t} \in \mathbb{R}^3$  for the location of a certain target at time  $t$ ). An observation  $z \in \mathbb{R}^4$  consists of noisy measurements of range, azimuth, elevation and Doppler signal. Note that the former three correspond to a noisy measurement of  $x$  in polar coordinates, and the latter one measures the projection of velocity onto the radial direction  $x$ .

The task of interest is estimation of  $x_{target,t}$  at any  $t$ . Denoting the corresponding point-estimate by  $\tilde{x}_{target,t}$ , our primary goal is to minimize  $MSE = \sum_{target} \sum_t (\tilde{x}_{target,t} - x_{target,t})^2$ . As a secondary goal, we also wish to minimize the negative-log-likelihood  $NLL = -\sum_{target} \sum_t \log l(x_{target,t} | D_{target,t}^P)$ . Here  $D_{target,t}^P$  is the distribution of the target location at time  $t$ , predicted using observations up to time  $t - 1$  (i.e., in terms of the KF, after the prediction step at time  $t - 1$ ), and  $l$  is the corresponding likelihood. While our case study focuses on tracking a single target at a time,  $NLL$  minimization is useful for matching observations to targets in the scope of the multi-target tracking problem.

The case study considers 5 types of tracking scenarios (*benchmarks*) and 4 variants of KF (*baselines*). For each benchmark and each baseline, we use the training data of the benchmark to produce one KF model with estimated noise parameters (Eq. (2)) and one with optimized parameters (see Section 4). We then evaluate the errors of both models on the test data of the benchmark (generated using different seeds than the training data). All experiments were run on eight i9-10900X CPU cores on a single Ubuntu machine.

Figures 2b,2c display a sample of trajectories in the simplest benchmark (*Toy*), which satisfies all KF assumptions except for a linear observation model  $H$ ; and in the *Free Motion* benchmark, which violates several assumptions (in a similar complexity as the scenario of Section 5). The other benchmarks are demonstrated in Appendix G. Figure 2a defines each of the 5 benchmarks more formally as a certain subset of the following properties:

- *anisotropic*: horizontal motion is more likely than vertical motion (otherwise motion direction is distributed uniformly).
- *polar*: radar noise is generated i.i.d in polar coordinates (otherwise noise is Cartesian i.i.d, which violates the physics of the system).
- *uncentered*: targets are not forced to concentrate close to the radar.
- *acceleration*: speed change is allowed.
- *turns*: non-straight motion is allowed.

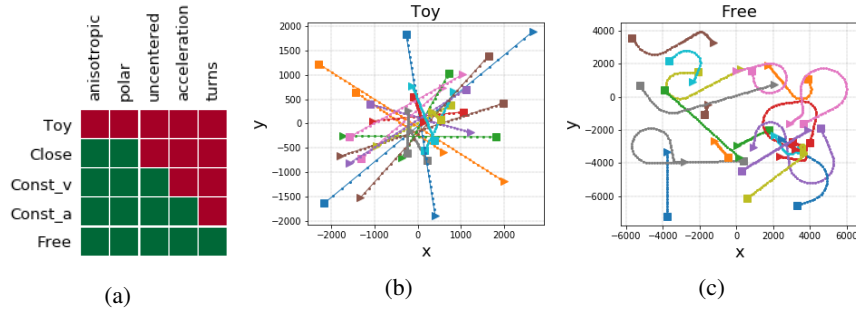


Figure 2: (a) Benchmarks names (rows) and the properties that define them (columns). Green means that the benchmark satisfies the property. (b,c) Samples of trajectories (projected onto XY plane) in Toy benchmark and Free Motion benchmark.

The 4 baselines differ from each other by using **either KF or EKF**, with **either Cartesian or polar coordinates** for representation of  $R$  (the rest of the system is always represented in Cartesian coordinates). In addition, as mentioned above, each baseline is tuned once by noise estimation and once by parameters optimization. See Appendix B for more details about the experimental setup.

We also repeat the experiment for the problem of tracking from video, using MOT20 dataset [Dendorfer et al., 2020] of real-world pedestrians, with train and test datasets taken from separated videos. For this problem we only consider a KF with Cartesian coordinates, since there is no polar component in the problem. Note that in contrast to radar tracking, video tracking enjoys a perfectly linear

Table 1: Summary of the out-of-sample errors of the various models over the various benchmarks. In the names of the models, "O" denotes optimized, "E" denotes extended, and "p" denotes polar (e.g., OEKFp is an *extended* KF with *polar* representation of  $R$  and *optimized* parameters). For each benchmark, the best estimated model and the best optimized model are marked. For KFp, we also consider an oracle-realization of  $R$  according to the true noise of the simulated radar in polar coordinates (available only in polar benchmarks). Note that (1) for any benchmark and any baseline, optimization yields lower error than estimation; and (2) this remains true even in the oracle variant, where the noise estimation is perfect.

| Benchmark | KF           | OKF   | KFp         | KFp (oracle) | OKFp         | EKF         | OEKF        | EKFp  | OEKFp |
|-----------|--------------|-------|-------------|--------------|--------------|-------------|-------------|-------|-------|
| Toy       | 151.7        | 84.2  | 269.6       | –            | 117.4        | <b>92.8</b> | <b>79.3</b> | 123.0 | 109.1 |
| Close     | 25.0         | 24.9  | <b>22.6</b> | 22.5         | <b>22.5</b>  | 26.4        | 26.2        | 24.5  | 24.1  |
| Const_v   | <b>90.2</b>  | 90.0  | 102.3       | 102.3        | <b>89.3</b>  | 102.5       | 101.5       | 112.7 | 102.2 |
| Const_a   | <b>107.5</b> | 101.7 | 118.4       | 118.3        | <b>100.5</b> | 110.0       | 107.5       | 126.0 | 108.9 |
| Free      | <b>125.9</b> | 118.8 | 145.6       | 139.3        | <b>118.1</b> | 135.8       | 122.1       | 149.3 | 120.2 |

observation model. This extends the scope of the experiments in terms of KF assumptions violations. See Appendix E for the detailed setup of the video tracking experiments.

### 3.2 Results

**Design decisions are not trivial:** Table 1 summarizes the tracking errors. The left column in each cell corresponds to a model with estimated (not optimized) parameters, and shows that in each benchmark, the errors strongly depend on the design decisions ( $R$ 's coordinates and whether to use EKF). In Toy benchmark, for example, EKF is the best design, since the observation model  $H$  is non-linear.

However, in other benchmarks the winning designs are arguably surprising:

1. Under non-isotropic motion direction, EKF is worse than KF in spite of the non-linear motion. It is possible that since the horizontal prior reduces the stochasticity of  $H$ , the advantage of EKF no longer justifies the instability of the derivative-based approximation.
2. Even when the observation noise is polar i.i.d, polar representation of  $R$  is not beneficial unless the targets are forced to concentrate close to the radar. It is possible that when the targets are distant, Cartesian coordinates have a more important role in expressing the horizontal prior of the motion.

Since the best variant of KF for each benchmark seems difficult to predict in advance, a practical system cannot rely on choosing the KF variant optimally, and rather has to be robust to this choice.

**Optimization is both beneficial and robust:** Table 1 shows that for any benchmark and any baseline, parameters optimization yielded smaller errors than noise estimation (over an out-of-sample test dataset). In addition, the variance between the baselines reduces under optimization, i.e., the optimization makes KF more robust to design decisions (which is also evident in Figure 9a in Appendix G).

We also studied the performance of a KF with a perfect knowledge of the noise covariance matrix  $R$ . Note that in the constant-speed benchmarks, the estimation of  $Q = 0$  is already very accurate, hence in these benchmarks the oracle-KF has a practically perfect knowledge of both noise covariances. Nonetheless, Table 1 shows that the oracle yields very similar results to a KF with estimated parameters. This indicates that the limitation of noise estimation in KF indeed comes from choosing the wrong goal, and not from estimation inaccuracy.

Figure 3 shows that parameters optimization provides significantly better predictions also in tracking from video, where it reduces the MSE by 18% (see Appendix E for more details).

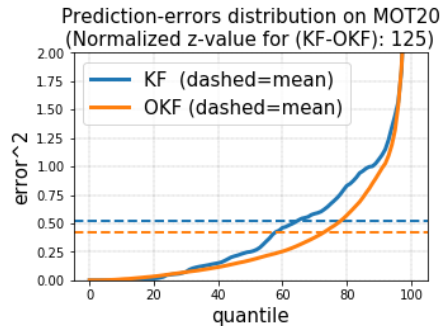


Figure 3: Prediction errors of KF and OKF on 1208 targets of the test data of MOT20 videos dataset. OKF is significantly more accurate.

**Diagnosis of KF sub-optimality in Toy scenario:** The source of the gap between estimated and optimized noise parameters can be studied through the simplest Toy benchmark, where the only violation of KF assumptions is the non-linear observation model  $H$ . Since the non-constant entries of  $H$  correspond to the Doppler observation, the non-linearity inserts uncertainty to the Doppler observation (in addition to the inherent observation noise). This increases Doppler’s effective noise in comparison to the location observation, as shown analytically in Appendix D. This explanation is consistent with Figure 4: the noise associated with Doppler is indeed increased by the optimization.

## 4 Optimization of SPD Matrices Using Cholesky Decomposition

As explained in Section 3,  $Q$  and  $R$  are usually considered as estimators of the noise. Even when viewed as parameters to optimize with respect to the filtering errors, they are still often determined by trial-and-error or by a grid-search [Formentin and Bittanti, 2014, Coskun et al., 2017]. The experiments in Section 3, however, required a more systematic optimization. To that end, we chose the Adam algorithm [Diederik P. Kingma, 2014], with respect to a loss function consisting of a linear combination of the squared filtering errors (MSE) and the negative log likelihood (NLL). Adam is a popular variant of the well-known gradient-descent algorithm, and has achieved remarkable results in many optimization problems in the field of machine learning in recent years, including in non-convex problems where local-minima exist.

Unfortunately, Adam cannot be applied directly to the entries of  $Q$  and  $R$  without ruining the symmetry and positive definiteness (SPD) properties of the covariance matrices. This difficulty often motivates optimization methods that avoid gradients [Abbeel et al., 2005], or even the restriction of  $Q$  and  $R$  to be diagonal [Li et al., 2019]. Indeed, Formentin and Bittanti [2014] pointed out that “since both the covariance matrices must be constrained to be positive semi-definite,  $Q$  and  $R$  are often parameterized as diagonal matrices”.

To allow Adam to optimize the non-diagonal  $Q$  and  $R$  we use the Cholesky decomposition [Horn and Johnson, 1985], which states that any SPD matrix  $A \in \mathbb{R}^{n \times n}$  can be written as  $A = LL^T$ , where  $L$  is lower-triangular with positive entries along its diagonal. The reversed claim is also true: for any lower-triangular  $L$  with positive diagonal,  $LL^T$  is SPD. Now consider the parameterization of  $A$  using the following  $\binom{n}{2} + n = \frac{n(n+1)}{2}$  parameters:  $\binom{n}{2}$  parameters correspond to  $\{L_{ij}\}_{1 \leq j < i \leq n}$ , and  $n$  parameters correspond to  $\{\log L_{ii}\}_{1 \leq i \leq n}$ . Clearly, the transformation from the parameters to the SPD matrix  $A = LL^T$  is continuous and outputs a SPD matrix for any realization of the parameters in  $\mathbb{R}^{n(n+1)/2}$ . Thus, we can apply Adam [Diederik P. Kingma, 2014] (or any other gradient-based method) to optimize these parameters without worrying about the SPD constraints. This approach, which is presented more formally in Appendix F and implemented in our `code`, was used for all the KF optimizations in this work.

The parameterization of covariance matrices using Cholesky decomposition was already suggested by Pinheiro and Bates [1996]. However, despite its simplicity, it is not commonly used for gradient-based optimization in SPD matrices in general, and to the best of our knowledge is not used at all for optimization of KF parameters in particular. Other methods were also suggested for SPD optimization, e.g., matrix-exponent [Tsuda et al., 2005] and projected gradient-descent with respect to the SPD cone [Tibshirani, 2015]. These methods require SVD-decomposition in every iteration, hence are computationally heavy, which may explain why they are not commonly used for tuning of KF. The parameterization derived from Cholesky decomposition only requires a single matrix multiplication, and thus is both efficient and easy to implement.

In addition to its efficiency, the suggested method is shown in Section 3 to be both effective and robust in tuning of KF. Furthermore, as it relies on standard tools from supervised machine learning, it is also applicable to high-dimensional parameters spaces. Consequentially, we believe that this

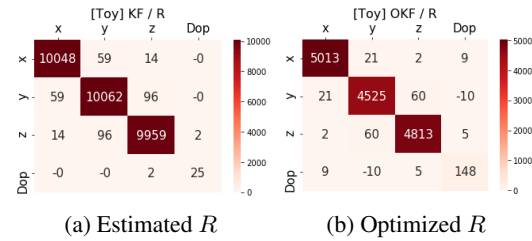


Figure 4: The covariance matrix  $R$  of the observation noise obtained in a (Cartesian) KF by noise estimation and by optimization, based on the dataset of the Toy benchmark. Note that the noise estimation is quite accurate for this benchmark, as the true variance of the noise is  $100^2$  for the positional dimensions and  $5^2$  for the Doppler signal.



method is capable of replacing noise estimation as the standard method for KF parameters tuning, in the scope of filtering problems with presence of ground-truth training data.

## 5 Neural Kalman Filter: Is the Non-linear Prediction Helpful?

A standard Kalman Filter for a tracking task assumes linear motion, as discussed in Section 2. In this section we introduce the *Neural Kalman Filter* tracking model (NKF), which uses LSTM networks to model non-linear motion, while keeping the framework of KF – namely, the probabilistic representation of the target’s state, and the separation between prediction and update steps.

Every prediction step, NKF uses a neural network model to predict the target’s acceleration  $a_t$  and the motion uncertainty  $Q_t$ . Every update step, another network predicts the observation uncertainty  $R_t$ . The predicted quantities are incorporated into the standard update equations of KF, which are stated in Figure 1. For example, the prediction step of NKF is:

$$x_{t+1}^P = Fx_t + 0.5a_t(\Delta t)^2$$

$$P_{t+1}^P = FP_tF^\top + Q_t$$

where  $F = F(\Delta t)$  is the constant-velocity motion operator, and  $a_t, Q_t$  are predicted by the LSTM (whose input includes the recent observation and the current estimated target’s state). Other predictive features were also attempted but failed to provide significant value, as described in Appendix B. Note that the neural network predicts the acceleration rather than directly predicting the location. This is intended to regularize the predictive model and to exploit the domain knowledge of kinematics.

After training NKF over a dataset of simulated targets with random turns and accelerations (see Appendix B for more details), we tested it on a separated test dataset. The test dataset is similar to the training dataset, with different seeds and an extended range of permitted accelerations. As shown in Figure 5, NKF significantly reduces the tracking errors compared to a standard KF.

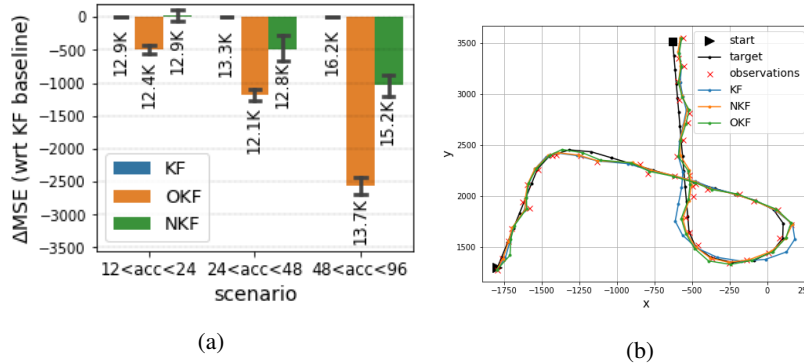


Figure 5: (a) Relative tracking errors (lower is better) with relation to a standard KF, over targets with different ranges of acceleration. The error-bars represent confidence intervals of 95%. The label of each bar represents the corresponding *absolute* MSE ( $\times 10^3$ ). In the training data, the acceleration was limited to 24–48, hence the other ranges measure generalization. While the Neural KF (NKF) is significantly better than the standard KF, its advantage is entirely eliminated once we optimize the KF (OKF). (b) A sample target and the corresponding models outputs (projected onto XY plane). The standard KF has a difficulty to handle some of the turns.

At this point, it seems that the non-linear architecture of NKF provides a better tracking accuracy in the non-linear problem of radar tracking. However, Figure 5 shows that by shifting the baseline from a naive KF to an optimized one, we *completely eliminate* the advantage of NKF, and in fact reduce the errors even further. In other words, the benefits of NKF come only from optimization and *not at all* from the expressive architecture. Hence, by overlooking the sub-optimality of noise estimation in KF, we would wrongly adopt the over-complicated model of NKF.

Note that the optimized variant of KF also generalizes quite well to targets with different accelerations than observed in the training. This indicates a certain robustness of the optimized KF to distributional shifts between the train and test data. Also note that while Figure 5 summarizes tracking errors, Figure 8 in Appendix G shows that the likelihood of the model is also improved by the optimized KF. High likelihood is important for the matching task in a multi-target tracking problem.



## 6 Related Work

**Noise estimation:** Estimation of the noise parameters in KF has been studied for decades. A popular framework for this problem is estimation from data of observations alone [Odelson et al., 2006, Feng et al., 2014, Park et al., 2019], since the ground-truth of the states is often unavailable in the data [Formentin and Bittanti, 2014]. In this work we assume that the ground-truth is available, where the current standard approach is to simply estimate the noise covariance matrix from the data [Odelson et al., 2006].

Many works addressed the problem of non-stationary noise estimation [Zanni et al., 2017, Akhlaghi et al., 2017]. However, as demonstrated in Sections 3,5, in certain cases stationary methods are highly competitive if tuned correctly – even in problems with complicated dynamics.

**Optimization:** In this work we apply gradient-based optimization to KF with respect to its errors. An optimization method that avoids gradients computation was already suggested in Abbeel et al. [2005]. In practice, "optimization" of KF is often handled manually using trial-and-error [Jamil et al., 2020], or using a grid-search over possible values of  $Q$  and  $R$  [Formentin and Bittanti, 2014, Coskun et al., 2017]. In other cases,  $Q$  and  $R$  are restricted to be diagonal [Li et al., 2019, Formentin and Bittanti, 2014].

Gradient-based optimization of SPD matrices in general was suggested in Tsuda et al. [2005] using matrix-exponents, and is also possible using projected gradient-descent [Tibshirani, 2015] – both rely on SVD-decomposition. In this work, we apply gradient-based optimization using the parameterization that was suggested in Pinheiro and Bates [1996], which requires a mere matrix multiplication, and thus is both efficient and easy to implement.

**Neural networks in filtering problems:** Section 5 presents a RNN-based extension of KF, and demonstrates how its advantage over the linear KF vanishes once the KF is optimized. The use of neural networks for non-linear filtering problems is very common in the literature, e.g., in online tracking prediction [Gao et al., 2019, Dan Iter, 2016, Coskun et al., 2017, fa Dai et al., 2020, Ullah et al., 2019], near-online prediction [Kim et al., 2018], and offline prediction [Liu et al., 2019b]. In addition, while Bewley et al. [2016] apply a KF for video tracking from mere object detections, Wojke et al. [2017] add to the same system a neural network that generates visual features as well. Neural networks were also considered for related problems such as data association [Liu et al., 2019a], model-switching [Deng et al., 2020], and sensors fusion [Sengupta et al., 2019].

In many works that consider neural networks for filtering problems, a variant of the KF is used as a baseline for comparison. However, while the parameters of the neural networks are normally optimized to minimize the filtering errors, the parameters tuning of the KF is sometimes ignored [Gao et al., 2019], sometimes based on noise estimation [fa Dai et al., 2020], and sometimes optimized in a limited manner as mentioned above [Jamil et al., 2020, Coskun et al., 2017]. Our findings imply that such a methodology yields over-optimistic conclusions, since the baseline is not optimized to the same level as the learning model.

See Appendix C for an extended discussion on related works.

## 7 Summary

Through a detailed case study, we demonstrated both analytically and empirically how fragile are the assumptions of the KF, and how the slightest violation of them may change the effective noise in the problem – leading to significant changes in the optimal noise parameters. We addressed this problem using optimization tools from supervised machine learning, and suggested how to apply them efficiently to the SPD parameters of KF. As this method was demonstrated accurate and robust in both radar tracking and video tracking, we recommended to use it as the default procedure for tuning of KF in presence of ground-truth data.

We also demonstrated one of the consequences of the use of sub-optimal KF: the common methodology of comparing learning filtering algorithms to classic variants of KF is misleading, as it essentially compares an optimized model to a non-optimized one. We argued that the baseline method should be optimized similarly to the researched one, e.g., using the optimization method suggested in this work.

## References

- Pieter Abbeel, Adam Coates, Michael Montemerlo, Andrew Ng, and Sebastian Thrun. Discriminative training of kalman filters. *Robotics: Science and systems*, pages 289–296, 06 2005. doi: 10.15607/RSS.2005.I.038.
- S. Akhlaghi, N. Zhou, and Z. Huang. Adaptive adjustment of noise covariance in kalman filter for dynamic state estimation. In *2017 IEEE Power Energy Society General Meeting*, pages 1–5, 2017. doi: 10.1109/PESGM.2017.8273755.
- Marcin Andrychowicz, Anton Raichuk, Piotr Stańczyk, Manu Orsini, Sertan Girgin, Raphael Marinier, Léonard Hussenot, Matthieu Geist, Olivier Pietquin, Marcin Michalski, Sylvain Gelly, and Olivier Bachem. What matters in on-policy reinforcement learning? a large-scale empirical study, 2020.
- S. T. Barratt and S. P. Boyd. Fitting a kalman smoother to data. In *2020 American Control Conference (ACC)*, pages 1526–1531, 2020. doi: 10.23919/ACC45564.2020.9147485.
- Alex Bewley, Zongyuan Ge, Lionel Ott, Fabio Ramos, and Ben Upcroft. Simple online and realtime tracking. In *2016 IEEE International Conference on Image Processing (ICIP)*, pages 3464–3468, 2016. doi: 10.1109/ICIP.2016.7533003.
- S. Blackman and R. Popoli. *Design and Analysis of Modern Tracking Systems*. Artech House Radar Library, Boston, 1999.
- W. R. Blanding, P. K. Willett, and Y. Bar-Shalom. Multiple target tracking using maximum likelihood probabilistic data association. In *2007 IEEE Aerospace Conference*, pages 1–12, 2007. doi: 10.1109/AERO.2007.353035.
- Chaw-Bing Chang and Keh-Ping Dunn. Radar tracking using state estimation and association: Estimation and association in a multiple radar system, 04 2019.
- Zhaozhong Chen et al. Kalman filter tuning with bayesian optimization, 2019.
- S. Kumar Chenna, Yogesh Kr. Jain, Himanshu Kapoor, Raju S. Bapi, N. Yadaiah, Atul Negi, V. Seshagiri Rao, and B. L. Deekshatulu. State estimation and tracking problems: A comparison between kalman filter and recurrent neural networks. *ICONIP*, 2004.
- Huseyin Coskun, Felix Achilles, Robert DiPietro, Nassir Navab, and Federico Tombari. Long short-term memory kalman filters: recurrent neural estimators for pose regularization. *ICCV*, 2017. URL [https://github.com/Seleucia/lstmkf\\_ICCV2017](https://github.com/Seleucia/lstmkf_ICCV2017).
- Philip Zhuang Dan Iter, Jonathan Kuck. Target tracking with kalman filtering, knn and lstms, 2016. URL <http://cs229.stanford.edu/proj2016/report/IterKuckZhuang-TargetTrackingwithKalmanFilteringKNNandLSTMs-report.pdf>.
- JP DeCruyenaere and HM Hafez. A comparison between kalman filters and recurrent neural networks. [*Proceedings 1992*] *IJCNN International Joint Conference on Neural Networks*, 4:247–251, 1992.
- Patrick Dendorfer, Hamid Rezafofighi, Anton Milan, Javen Shi, Daniel Cremers, Ian Reid, Stefan Roth, Konrad Schindler, and Laura Leal-Taixé. Mot20: A benchmark for multi object tracking in crowded scenes, 2020. URL <https://motchallenge.net/data/MOT20/>.
- Lichuan Deng, Da Li, and Ruifang Li. Improved IMM Algorithm based on RNNs. *Journal of Physics Conference Series*, 1518:012055, April 2020. doi: 10.1088/1742-6596/1518/1/012055.
- Jimmy Ba Diederik P. Kingma. Adam: A method for stochastic optimization, 2014. URL <https://arxiv.org/abs/1412.6980>.
- Logan Engstrom, Andrew Ilyas, Shibani Santurkar, Dimitris Tsipras, Firdaus Janoos, Larry Rudolph, and Aleksander Madry. Implementation matters in deep policy gradients: A case study on ppo and trpo. *ICLR*, 2019. URL <https://openreview.net/pdf?id=r1etN1rtPB>.
- Hai fa Dai, Hong wei Bian, Rong ying Wang, and Heng Ma. An ins/gnss integrated navigation in gnss denied environment using recurrent neural network. *Defence Technology*, 16(2):334–340, 2020. ISSN 2214-9147. doi: <https://doi.org/10.1016/j.dt.2019.08.011>. URL <https://www.sciencedirect.com/science/article/pii/S2214914719303058>.

- B. Feng, M. Fu, H. Ma, Y. Xia, and B. Wang. Kalman filter with recursive covariance estimation—sequentially estimating process noise covariance. *IEEE Transactions on Industrial Electronics*, 61(11):6253–6263, 2014. doi: 10.1109/TIE.2014.2301756.
- Simone Formentin and Sergio Bittanti. An insight into noise covariance estimation for kalman filter design. *IFAC Proceedings Volumes*, 47(3):2358–2363, 2014. ISSN 1474-6670. doi: <https://doi.org/10.3182/20140824-6-ZA-1003.01611>. URL <https://www.sciencedirect.com/science/article/pii/S1474667016419646>. 19th IFAC World Congress.
- C. Gao, H. Liu, S. Zhou, H. Su, B. Chen, J. Yan, and K. Yin. Maneuvering target tracking with recurrent neural networks for radar application. *2018 International Conference on Radar (RADAR)*, pages 1–5, 2018.
- Chang Gao, Junkun Yan, Shenghua Zhou, Bo Chen, and Hongwei Liu. Long short-term memory-based recurrent neural networks for nonlinear target tracking. *Signal Processing*, 164, 05 2019. doi: 10.1016/j.sigpro.2019.05.027.
- Google Scholar. Citations since 2017: "a new approach to linear filtering and prediction problems", 2021. URL [https://scholar.google.com/scholar?as\\_ylo=2017&hl=en&as\\_sdt=2005&sciodt=0,5&cites=5225957811069312144&scipsc=](https://scholar.google.com/scholar?as_ylo=2017&hl=en&as_sdt=2005&sciodt=0,5&cites=5225957811069312144&scipsc=).
- Peter Henderson, Riashat Islam, Philip Bachman, Joelle Pineau, Doina Precup, and David Meger. Deep Reinforcement Learning that Matters. *arXiv preprint arXiv:1709.06560*, 2017. URL <https://arxiv.org/pdf/1709.06560.pdf>.
- Sepp Hochreiter and Jurgen Schmidhuber. Long short-term memory. *Neural Computation*, 1997. URL <https://direct.mit.edu/neco/article/9/8/1735/6109/Long-Short-Term-Memory>.
- R. A. Horn and C. R. Johnson. *Matrix Analysis*. Cambridge University Press, 1985.
- Jeffrey Humpherys, Preston Redd, and Jeremy West. A fresh look at the kalman filter. *SIAM Review*, 54(4):801–823, 2012. doi: 10.1137/100799666.
- Faisal Jamil et al. Toward accurate position estimation using learning to prediction algorithm in indoor navigation. *Sensors*, 2020.
- S. J. Julier and J. K. Uhlmann. Unscented filtering and nonlinear estimation. *Proceedings of the IEEE*, 92(3):401–422, 2004. doi: 10.1109/JPROC.2003.823141.
- R. E. Kalman. A New Approach to Linear Filtering and Prediction Problems. *Journal of Basic Engineering*, 82(1):35–45, 03 1960. ISSN 0021-9223. doi: 10.1115/1.3662552. URL <https://doi.org/10.1115/1.3662552>.
- Chanho Kim, Fuxin Li, and James M. Rehg. Multi-object tracking with neural gating using bilinear lstm. *ECCV*, September 2018.
- Yaakov Bar-Shalom X.-Rong Li Thiagalingam Kirubarajan. *Estimation with Applications to Tracking and Navigation: Theory, Algorithms and Software*. John Wiley and Sons, Inc., 2002. doi: 10.1002/0471221279.
- Harold W Kuhn. The hungarian method for the assignment problem. *Naval research logistics quarterly*, 2(1-2):83–97, 1955.
- Tony Lacey. Tutorial: The kalman filter, 1998. URL "<http://web.mit.edu/kirtley/kirtley/binlustuff/literature/control/Kalmanfilter.pdf>".
- S. Li, C. De Wagter, and G. C. H. E. de Croon. Unsupervised tuning of filter parameters without ground-truth applied to aerial robots. *IEEE Robotics and Automation Letters*, 4(4):4102–4107, 2019. doi: 10.1109/LRA.2019.2930480.
- M. Linderoth, K. Soltesz, A. Robertsson, and R. Johansson. Initialization of the kalman filter without assumptions on the initial state. In *2011 IEEE International Conference on Robotics and Automation*, pages 4992–4997, 2011. doi: 10.1109/ICRA.2011.5979684.
- Hu Liu et al. Kalman filtering attention for user behavior modeling in ctr prediction. *NeurIPS*, 2020.

- Huajun Liu, Hui Zhang, and Christoph Mertz. Deepda: Lstm-based deep data association network for multi-targets tracking in clutter. *CoRR*, abs/1907.09915, 2019a. URL <http://arxiv.org/abs/1907.09915>.
- Jingxian Liu, Zulin Wang, and Mai Xu. Deepmtt: A deep learning maneuvering target-tracking algorithm based on bidirectional lstm network. *Information Fusion*, 53, 06 2019b. doi: 10.1016/j.inffus.2019.06.012.
- E. Mazor, A. Averbuch, Y. Bar-Shalom, and J. Dayan. Interacting multiple model methods in target tracking: a survey. *IEEE Transactions on Aerospace and Electronic Systems*, 34(1):103–123, 1998.
- Dominic A. Neu, Johannes Lahann, and Peter Fettke. A systematic literature review on state-of-the-art deep learning methods for process prediction. *CoRR*, abs/2101.09320, 2021. URL <https://arxiv.org/abs/2101.09320>.
- Brian Odelson, Alexander Lutz, and James Rawlings. The autocovariance least-squares method for estimating covariances: Application to model-based control of chemical reactors. *Control Systems Technology, IEEE Transactions on*, 14:532 – 540, 06 2006. doi: 10.1109/TCST.2005.860519.
- Sebin Park et al. Measurement noise recommendation for efficient kalman filtering over a large amount of sensor data. *Sensors*, 2019.
- Dong-liang Peng and Yu Gu. Imm algorithm for a 3d high maneuvering target tracking. *International Conference in Swarm Intelligence*, pages 529–536, 06 2011. doi: 10.1007/978-3-642-21524-7\_65.
- José C. Pinheiro and Douglas M. Bates. Unconstrained parameterizations for variance-covariance matrices. *Statistics and Computing*, 6:289–296, 1996.
- B. Ristic, S. Arulampalam, and N. Gordon. *Beyond the Kalman Filter: Particle Filters for Tracking Applications*. Artech house Boston, 2004.
- David E. Rumelhart et al. Learning representations by back-propagating errors. *Nature*, 1986. URL <https://www.nature.com/articles/323533a0>.
- A. Sengupta, F. Jin, and S. Cao. A dnn-lstm based target tracking approach using mmwave radar and camera sensor fusion. *2019 IEEE National Aerospace and Electronics Conference (NAECON)*, pages 688–693, 2019. doi: 10.1109/NAECON46414.2019.9058168.
- D. J. Thomson. Jackknifing multiple-window spectra. In *Proceedings of ICASSP '94. IEEE International Conference on Acoustics, Speech and Signal Processing*, volume vi, pages VI/73–VI/76 vol.6, 1994. doi: 10.1109/ICASSP.1994.389899.
- Ryan Tibshirani. Proximal gradient descent and acceleration, 2015. URL <https://www.stat.cmu.edu/~ryantibs/convexopt-F15/lectures/08-prox-grad.pdf>.
- Koji Tsuda, Gunnar Rätsch, and Manfred K. Warmuth. Matrix exponentiated gradient updates for on-line learning and bregman projection. *Journal of Machine Learning Research*, 6(34):995–1018, 2005. URL <http://jmlr.org/papers/v6/tsuda05a.html>.
- Israr Ullah, Muhammad Fayaz, and DoHyeun Kim. Improving accuracy of the kalman filter algorithm in dynamic conditions using ann-based learning module. *Symmetry*, 11(1), 2019. ISSN 2073-8994. doi: 10.3390/sym11010094. URL <https://www.mdpi.com/2073-8994/11/1/94>.
- Ashish Vaswani et al. Attention is all you need. *NeurIPS*, 2017.
- E. Wan. Sigma-point filters: An overview with applications to integrated navigation and vision assisted control. *IEEE*, pages 201–202, 2006. doi: 10.1109/NSSPW.2006.4378854.
- E. A. Wan and R. Van Der Merwe. The unscented kalman filter for nonlinear estimation. *Proceedings of the IEEE 2000 Adaptive Systems for Signal Processing, Communications, and Control Symposium (Cat. No.00EX373)*, pages 153–158, 2000. doi: 10.1109/ASSPCC.2000.882463.
- Nicolai Wojke, Alex Bewley, and Dietrich Paulus. Simple online and realtime tracking with a deep association metric. In *2017 IEEE International Conference on Image Processing (ICIP)*, pages 3645–3649, 2017. doi: 10.1109/ICIP.2017.8296962.

L. Zanni, J. Le Boudec, R. Cherkaoui, and M. Paolone. A prediction-error covariance estimator for adaptive kalman filtering in step-varying processes: Application to power-system state estimation. *IEEE Transactions on Control Systems Technology*, 25(5):1683–1697, 2017. doi: 10.1109/TCST.2016.2628716.

Paul Zarchan and Howard Musoff. *Fundamentals of Kalman Filtering: A Practical Approach*. American Institute of Aeronautics and Astronautics, 2000.

## Contents

|          |  |           |
|----------|--|-----------|
| <b>1</b> | <b>Introduction</b>  | <b>1</b>  |
| <b>2</b> | <b>Preliminaries and Problem Setup</b>                             | <b>3</b>  |
| <b>3</b> | <b>Kalman Filter Configuration and Optimization: a Case Study</b>  | <b>4</b>  |
| <b>4</b> | <b>Optimization of SPD Matrices Using Cholesky Decomposition</b>   | <b>7</b>  |
| <b>5</b> | <b>Neural Kalman Filter: Is the Non-linear Prediction Helpful?</b> | <b>8</b>  |
| <b>6</b> | <b>Related Work</b>  | <b>9</b>  |
| <b>7</b> | <b>Summary</b>   | <b>9</b>  |
| <b>A</b> | <b>Preliminaries: Extended</b>                                     | <b>15</b> |
| <b>B</b> | <b>Problem Setup and Implementation Details</b>                    | <b>17</b> |
| <b>C</b> | <b>Related Work: Extended</b>                                      | <b>19</b> |
| <b>D</b> | <b>Estimation vs. Optimization Analysis on Toy Benchmark</b>       | <b>20</b> |
| <b>E</b> | <b>Optimized Kalman Filter for Video Tracking</b>                  | <b>21</b> |
| <b>F</b> | <b>Cholesky Gradient Optimization</b>                              | <b>22</b> |
| <b>G</b> | <b>Detailed Results</b>  | <b>23</b> |

## A Preliminaries: Extended

### A.1 Multi-target Radar Tracking

In the problem of multi-target radar tracking, noisy observations (or *detections*) of aerial objects (or *targets*) are received by the radar and are used to keep track of the objects. In standard radar sensors, the signal of an observation includes the target range and direction (which can be converted into location coordinates  $x, y, z$ ), as well as the Doppler shift (which can be converted into the projection of velocity  $v_x, v_y, v_z$  onto the location vector).

The problem consists of observations-trackers assignment, where each detection of a target should be assigned to the tracker representing the same target; and of location estimation, where the location of each target is estimated at any point of time according to the observations [Chang and Dunn, 2019]. In the fully online setup of this problem, the assignment of observations is done once they are received, before knowing the future observations on the targets (though observations of different targets may be received simultaneously); and the location estimation at any time must depend only on previously received observations.

**Assignment problem:** The assignment problem can be seen as a one-to-one matching problem in the bipartite graph of existing trackers and newly-received observations, where the edge between a tracker and an observation represents "how likely the observation  $z_j$  is for the tracker  $trk_i$ ". In particular, if the negative-log-likelihood is used for edges weights, then the total cost of the match represents the total likelihood (under the assumption of observations independence):

$$C(\text{match}) = \sum_{(i,j) \in \text{match}} -\log P(z_j | trk_i) = -\log \prod_{(i,j) \in \text{match}} P(z_j | trk_i) \quad (3)$$

The assignment problem can be solved using standard polynomial-time algorithms such as the Hungarian algorithm [Kuhn, 1955]. However, the assignment can only be as good as the likelihood information fed to the algorithm. This is a major motivation for trackers that maintain probabilistic representation of the target, rather than a merely point estimate of the location. A common example for such a tracking mechanism is the Kalman filter discussed below.

### A.2 Kalman Filter

Kalman Filter (KF) is a widely-used method for linear filtering and prediction originated in the 1960s [Kalman, 1960], with applications in many fields [Zarchan and Musoff, 2000] including object tracking [Kirubarajan, 2002]. The classic model keeps an estimate of the monitored system state (e.g., location and velocity), represented as the mean  $x$  and covariance  $P$  of a normal distribution (which uniquely determine the PDF of the distribution). The mechanism (see Figure 1) alternately applies a *prediction step*, where a linear model  $x := Fx$  predicts the next state; and an *update step* (also termed *filtering step*), where the information of a new observation  $z$  is incorporated into the estimation (after a transformation  $H$  from the observation space to the state space).

Note that KF compactly keeps our knowledge about the monitored target at any point of time, which allows us to estimate both whether a new observation corresponds to the currently monitored target, and what the state of the system currently is. However, KF strongly relies on several assumptions:

1. **Linearity:** both the state-transition of the target  $f$  and the state-observation transformation  $h$  are assumed to be linear, namely,  $f(x) = F \cdot x$  and  $h(x) = H \cdot x$ . Note that the Extended KF described below, while not assuming linearity, still assumes known models for transition and observation.
2. **Normality:** both state-transition and state-observation are assumed to have a Gaussian noise with covariance matrices  $Q$  and  $R$  respectively. As a result, the estimates of the state  $x$  and its uncertainty  $P$  also correspond to the mean and covariance matrix of a Normal distribution representing the information regarding the target location.
3. **Known model:**  $F, Q, H, R$  are assumed to be known.

While  $F$  and  $H$  are usually determined manually according to domain knowledge, the noise model parameters  $R, Q$  are often estimated from data (as long as the true states are available in the



data). Specifically, they are often estimated from the sample covariance matrix of the noise:  $R := Cov(Z - HX)$ ,  $Q := Cov(\Delta X) = Cov(\{x_{t+1} - Fx_t\}_t)$  [Lacey, 1998].

Two non-linear extensions of KF – *Extended Kalman Filter* (EKF) [Julier and Uhlmann, 2004] and *Unscented Kalman Filter* (UKF) [Wan and Van Der Merwe, 2000] – are also very popular in problems of non-linear state estimation and navigation [Wan, 2006]. EKF replaces the linear prediction ( $F$ ) and observation ( $H$ ) models with non-linear known models  $f$  and  $h$ , and essentially runs a standard KF with the local linear approximations  $F = \frac{\partial f}{\partial x}|_{x_t}$ ,  $H = \frac{\partial h}{\partial x}|_{x_t}$ , updating in every step  $t$ . UKF does not pass the state distribution  $x, P$  through the motion equations as a whole distribution, since such distribution transformation is unknown for general nonlinear state-transition. Instead, it samples *sigma points* from the original Gaussian distribution, passes each point through the nonlinear transition, and uses the resulting points to estimate the new Gaussian distribution. *Particle filters* go farther and do not bother to carry a Gaussian PDF: instead, the points themselves (*particles*) can be seen as representatives of the distribution.

Whether linear or not, a single simple model is hardly enough to represent the motion of any aerial target. A common approach is to maintain a switching model that repeatedly chooses between several mode, each controlled by a different motion model. Common simple models the Constant Velocity (CV), Constant Acceleration (CA), and Coordinated Turn Left or Right (CTL and CLR). Note that in all these models the prediction operator  $F$  is linear. A popular switching mechanism is the *Interactive Multiple Model* (IMM) [Mazor et al., 1998], which relies on knowing the transition-probabilities between the various modes.

In addition to the challenge of predicting mode-transitions, the standard models in use are often too simple to represent the motions of modern and highly-maneuvering targets, such as certain unmanned aerial vehicles, drones and missiles. Many approaches have been recently attempted to improve tracking of such objects, as discussed in Section C.

### A.3 Recurrent Neural Networks

*Neural networks* (NN) are parametric functions, usually constructed as a sequence of matrix-multiplications with some non-linear differentiable transformation between them. NNs are known to be able to approximate complicated functions, given that the right parameters are chosen. Optimization of the parameters of NNs is a field of vast research for decades, and usually relies on gradient-based methods, that is, calculating the errors of the NN with relation to some training-data of inputs and their desired outputs, deriving the errors with respect to the network’s parameters, and moving the parameters against the direction of the gradient.

*Recurrent neural networks* (RNN) [Rumelhart et al., 1986] are NN that are intended to be iteratively fed with sequential data samples, and that pass information (*hidden state*) during the sequential processing. Every iteration, the hidden state is fed to the next instance of the network as part of its input, along with the new data sample. *Long Short Term Memory* (LSTM) [Hochreiter and Schmidhuber, 1997] is an example to an architecture of RNN. It is particularly popular due to the linear flow of the hidden state over iterations, which allows to capture memory for relatively long term.

### A.4 Noise Dependence by Change of Coordinates

One of the violations of the KF assumptions in Section 3 is the non-i.i.d nature of the noise. The interest in this violation is increased by the fact that the noise is simulated in an i.i.d manner, which makes the violation non-trivial to notice.

The violation is caused by the difference of coordinates: while the state of the target is represented in Cartesian coordinates, the noise is generated in polar ones. As a result, polar dimensions with higher noise are assigned to the same Cartesian dimensions in consecutive time-steps, creating dependence between the noise in these time-steps in Cartesian coordinates.

For example, consider a radar with a noiseless angular estimation (i.e., all the noise is radial), and consider a low target (in the same height of the radar). Clearly, most of the noise will be in the XY plane – both in the current time-steps and in the following ones (until the target gets far from the plane). In other words, the noise in the following time-steps statistically-depends on the current time-step, and is not i.i.d.

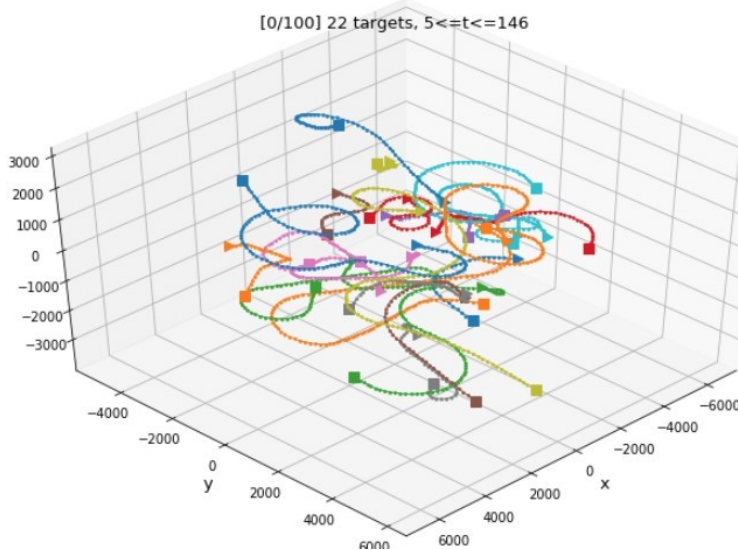


Figure 6: A sample of targets trajectories.

## B Problem Setup and Implementation Details

**Code:** The code for this work is available [here](#), and naturally contains implementation details that may be missing in the descriptions below.

**Targets simulation:** Our simulated dataset consists of episodes of tens to hundreds of seconds. Each episode contains around 20 targets. Each target appears at a certain point of time, has certain acceleration and speed ranges, and alternately performs straight motions (in constant speed or with acceleration) and turns (horizontally or vertically) until it disappears. The time progresses in discrete time-steps of size  $dt$ . The space is assumed to be 3D and homogeneous (no ground).

The randomization in an episode is expressed through the number of targets, each target’s acceleration and speed ranges, target appearing time, initial target state, number of turns, directions of turns (left/right/up/down), length of turns, length of straight intervals, whether accelerating in straight intervals and what the acceleration is.

**Radar simulation:** Every time-step, the radar generates detections of the available targets. Each detection contains location information  $(x, y, z)$  and a Doppler measurement corresponding to the projection of velocity onto the location vector. Each detection has an additive i.i.d Gaussian noise in polar coordinates, i.e., range, azimuth, elevation, and Doppler. The radar itself is assumed to be a singular point located in the origin  $(0, 0, 0)$ . Recall that we assume a homogeneous space with no ground.

**Tracking test framework:** The predictive models (*trackers*) can be tested in a mere prediction framework (where each target is tested by itself), or in a full tracking framework (where multiple targets are tracked simultaneously). In the latter, we use a tracking system (*solver*) consisting of a matcher and multiple trackers. Every time-step during a test episode, the solver runs the following procedures:

1. **Observe:** receive observations from the radar.
2. **Assign:** use the matcher (based on the standard Hungarian Algorithm [Kuhn, 1955], with relation to the corresponding trackers’ likelihood functions) to assign observations to trackers; create a new tracker for any unassigned observation; and delete any tracker whose target was not observed for several time-steps.
3. **Update:** update the location estimation of the trackers using the newly-assigned observations.

4. **Predict:** predict the target location in the next time-step (to allow more accurate assignment of the next batch of observations).

In the scope of this work we are mainly interested in the tracker module. Note that the tracker affects the matching accuracy through the likelihoods it feeds to the matcher; and affects the estimation accuracy directly in the prediction and update operations. To solve both matching and estimation tasks, the tracker is required to provide a good probabilistic model of the target location (namely, a PDF of the location) in addition to a point estimate.

We measure the estimation accuracy using the standard Mean Square Error (MSE) of the target location after the update step. For matching accuracy, for each target we consider the tracker that covers most of the target’s observations, and count the percent of observations assigned to that tracker.

**Trackers:** To support the procedures described above, a tracker must implement prediction and update steps, as well as exporting the current point estimate of the target location and the likelihood of any observation whenever queried.

All the trackers in this work are conceptually based on Kalman Filter (described in Section A.2). The following elements characterize the exact nature of the tracker:

1. **KF/EKF:** the difference is in the observation model  $H$ , as explained in Section A.2.
2. **Coordinates for representation of the observation noise  $R$ :** while we represent the state in Cartesian coordinates  $((x, y, z, vx, vy, vz)^\top)$  and measure the errors accordingly, the natural coordinates for the noise of the radar are polar, as the observation errors are simulated independently for range, azimuth, elevation and Doppler. In particular, in Cartesian coordinates the errors are not independent, hence  $R$  is not inherently constant. When implementing  $R$  in polar coordinates, we have to transform it to Cartesian coordinates every time-step according to the recent observation.
3. **Determining the noise parameters  $Q, R$  by estimation/optimization:** by estimation of the noise we mean  $Q = Cov(X_{t+1} - FX_t), R = Cov(Z_t - HX_t)$  over the training data  $\{X_t, Z_t\}$ . By optimization we mean that  $R \in \mathbb{R}^{4 \times 4}, Q \in \mathbb{R}^{6 \times 6}$  are intended to minimize the loss of the predictions over the training data. Note that in the optimization, we represent  $R, Q$  using lower-triangular decomposition so that both matrices remain SPD.
4. **Acceleration prediction:** replace the linear motion model  $Fx$  with  $Fx + 0.5a \cdot dt^2$ , where  $a$  is predicted using a LSTM that receives the observations and estimated states as recurrent inputs.
5.  **$Q$  prediction:** dynamically predict the motion model noise  $Q$  using an LSTM. We use the same LSTM as for  $a$ , except for the head layer that outputs  $Q$  itself. For simplicity, we assume that  $Q$  is diagonal when dynamically predicted.
6.  **$R$  prediction:** dynamically predict the observation noise  $R$  using a neural network that receives the recent observations and estimated states as inputs. For simplicity, we assume that  $R$  is diagonal when dynamically predicted.
7.  **$H$  prediction:** the observation model  $z = h(x)$  of a radar is a non-linear function of  $x$ . Extended KF handles this through a linear approximation of  $h$  around the currently-estimated state  $x$ . By  $H$ -prediction, we aim to learn to choose  $H$  dynamically in an optimal way to improve the tracking errors.
8. **Mixture-of-Gaussians representation:** KF assumes Gaussian errors (in prediction and observation), hence the distribution of the state is always normal, which is somewhat limiting. We try to represent the distribution as a mixture of Gaussians (i.e., a linear combination of a few Gaussians). The Gaussians are intended to correspond to possible modes of motion (e.g., constant speed vs. a turn), and thus can predict the dynamic acceleration (see above) differently from each other. In addition, the amplitude of each Gaussian (i.e., the probability assigned to it) is predicted every step along with the accelerations.

Optimization of the noise parameters ( $R, Q$ ) was implemented as part of the Optimized Kalman Filter (OKF) described in Section 3. This feature was found to make the tracker both more accurate and more robust to design choices such as KF vs. EKF or coordinates of  $R$  as described above. A neural-network-based Dynamic prediction of acceleration and noise was implemented as part of the Neural Kalman Filter (NKF) described in Section 5.

The last two features in the list failed to provide successful results: dynamic prediction of  $H$  yielded very unstable predictions, and a mixture representation had insignificant effects on the prediction. Furthermore, beyond 2 Gaussians in the mixture, it seemed that any additional Gaussian became practically inactive, with amplitude being constantly near zero.

**Training:** Training has to be applied to certain trackers, such as OKF (which optimizes  $R$  and  $Q$ ) and NKF (which optimizes the dynamic prediction of  $R$ ,  $Q$  and the acceleration). The training dataset consists of targets, each containing a sequence of states (locations and velocities) along with a sequence of observations. In particular, the true state (location and velocity) of a target is assumed to be known and available to learn from. This can be achieved either by a simulated environment or by internal targets sensors (e.g., GPS) in a physical environment. Note that the training dataset considers the targets independently of each other, and does not refer to the notion of episodes with possibly-simultaneous targets. Targets assignment in such episodes is handled by the Hungarian algorithm as mentioned above. The test dataset differs from the training dataset in the seeds used to generate the trajectories and the observations, and in certain experiments also in some configuration parameters such as the permitted range of acceleration.

Every epoch of training goes over each training target once. In the beginning of each epoch, batches of 10 targets are randomly drawn. Every training step corresponds to a single batch, where the training loss is aggregated additively over the targets in the batch and over the time-steps of each target. The training loss is a weighted average of (1) the Negative-Log-Likelihood (NLL) of the true state with relation to the estimated state, after each prediction step; and (2) the Mean Square Error (MSE) of the estimated location after the update step.

The optimization is done using Adam [Diederik P. Kingma, 2014] algorithm with learning rate of 0.01 and no weight-decay. The learning rate is reduced by 50% every 150 training steps.

## C Related Work: Extended

**Kalman Filter parameters tuning:** Estimation of the noise parameters in KF has been researched for decades. A popular framework for this problem is estimation from data of observations  $\{z\}$  alone [Odelson et al., 2006, Feng et al., 2014, Park et al., 2019], since the ground-truth of the states  $\{x\}$  is often unavailable in the data [Formentin and Bittanti, 2014]. In this work we assume that the ground-truth is available.

Many works addressed the problem of non-stationary noise estimation [Zanni et al., 2017, Akhlaghi et al., 2017]. However, as demonstrated in Sections 3,5, in certain cases stationary methods are highly competitive if tuned correctly – even in problems with complicated dynamics.

Optimization of KF parameters with respect to tracking errors was already suggested in Abbeel et al. [2005], using a method that avoids gradients computation. In practice, "optimization" of KF parameters with respect to the errors is often handled manually using trial-and-error [Jamil et al., 2020], or using a grid-search over possible values of  $Q$  and  $R$  [Formentin and Bittanti, 2014, Coskun et al., 2017]. Alternatively, the optimization is often simplified by restricting  $Q$  and  $R$  to be diagonal (e.g., see the experiments in Barratt and Boyd [2020] and Li et al. [2019]). Formentin and Bittanti [2014] pointed out explicitly that "since both the covariance matrices must be constrained to be positive semi-definite,  $Q$  and  $R$  are often parameterized as diagonal matrices".

Gradient-based optimization of SPD matrices in general was suggested in Tsuda et al. [2005] using matrix-exponents, and is also possible using projected gradient-descent [Tibshirani, 2015] – both rely on SVD-decomposition. In this work, we apply gradient-based optimization using the parameterization that was suggested in Pinheiro and Bates [1996], which requires a mere matrix multiplication, and thus is both efficient and easy to implement.

**Neural networks for tracking:** While comparison between RNN and KF goes back to DeCruyenaere and Hafez [1992], Chenna et al. [2004], the contribution of neural networks to non-linear motion tracking has been widely researched mostly in recent years, in the context of both radar and other sensors. Liu et al. [2019b] focus on an offline framework, where a bidirectional LSTM receives a full, normalized trajectory as an input, and improves the target locations estimations of a UKF in a 2-dimensional space. The LSTM is trained to predict the residual errors of the UKF. Kim et al. [2018] focus on a "near-online" framework, where assignment of an observation is decided after

looking ahead a certain number of observations. They operate in the visual domain, incorporate both visual and motion information together to make decisions, and suggest a new variant of LSTM, where the hidden state  $h$  interacts with the new input  $x$  through the multiplication  $hx$  rather than linear combination of the two, and thus can be interpreted as a dynamic model rather than hidden memory.

Gao et al. [2018] focus on an online framework, similarly to our work, where assignments and estimations are done immediately with the receipt of the observations. For the private case of a one-dimensional recurrent input signal, they use two LSTMs for estimation of the target location – one for the prediction step and one for the update step – to achieve improved estimation. Gao et al. [2019] expand this work and learn to predict both the location estimate and its (one-dimensional) variance according to the negative-log-likelihood loss, which yields similar accuracy but provides uncertainty estimation. Dan Iter [2016] consider online tracking of single vehicles on the 2-dimensional video screen of a vehicle camera (the KITTI object tracking benchmark). Since they assume zero observation error, they focus on prediction error optimization. Their LSTM yields a better point-prediction than KF, but does not improve the end-to-end tracking, which they hypothesize that could be caused by insufficient uncertainty estimation. Coskun et al. [2017] suggest a combination of LSTM and KF for the task of human pose estimation, learned on basis of the square estimation-errors. In particular, three LSTM modules are used to predict the parameters  $F, Q, R$  of a KF.

Liu et al. [2019a] train an LSTM for data association, i.e., the assignment task. Sengupta et al. [2019] address the problem of sensors fusion using a deep neural network. They incorporate information from a monocular camera and a mmWave radar, and show how to handle failures in either of the sensors. Deng et al. [2020] consider standard models as building blocks for IMM, and replace the mode-transition matrix with an LSTM that estimates the transition probabilities dynamically. Peng and Gu [2011] replace the standard building blocks of IMM with modes that are dedicatedly-designed to track highly-maneuvering targets.

A combination of KF with attention models [Vaswani et al., 2017] was also suggested [Liu et al., 2020] in the context of click-through rate prediction in e-commerce, where vital information for prediction may be concentrated in certain time-steps on which the model should focus.

## D Estimation vs. Optimization Analysis on Toy Benchmark

Section 3 demonstrates that the optimal noise parameters in KF often differ from the covariance of the noise. Here we analyze this effect for the private case of the Toy benchmark, where all KF assumptions (Definition 2.1) hold – except for the non-linear observation model  $H(X)$ .

The observation model  $H$  in KF satisfies

$$Z_t = H(X_t) \cdot X_t + \nu_t \quad (4)$$

where  $Z_t$  is the observation at time  $t$ ,  $X_t$  is the system’s state,  $H(X_t)$  is a transformation between them, and  $\nu_t \sim N(0, R)$  is the i.i.d observation noise. Under KF assumptions, the observation model is linear, i.e.,  $H(X) \equiv H_0$ . However, this is not the case in a Doppler radar, where the Doppler signal is the radial projection of the velocity and depends on the target location:

$$H(X) = \begin{pmatrix} 1 & & & & & \\ & 1 & & & & \\ & & 1 & & & \\ & & & x/r & y/r & z/r \end{pmatrix} \in \mathbb{R}^{4 \times 6}$$

where  $X = (x, y, z, u_x, u_y, u_z)^\top$ ,  $r = \sqrt{x^2 + y^2 + z^2}$ , and the observation is  $Z = (z_x, z_y, z_z, z_{Doppler})^\top$ .

Since the true  $X$  is unknown to the KF,  $H(X)$  is approximated by  $\tilde{H}$  that relies on a mere estimation of  $x, y, z$ . In particular, using the notation  $\hat{x} := x/r$  (and similarly for  $\hat{y}, \hat{z}$ ), we can write

$$\tilde{H} = \begin{pmatrix} 1 & & & & & \\ & 1 & & & & \\ & & 1 & & & \\ & & & \hat{x} + d\hat{x} & \hat{y} + d\hat{y} & \hat{z} + d\hat{z} \end{pmatrix}$$

where  $d\hat{x}, d\hat{y}, d\hat{z}$  are the corresponding estimation errors. Note that in the private case where  $x, y, z$  are estimated by  $z_x, z_y, z_z$ , these errors coincide with the corresponding entries of  $\nu$  (up to the normalization by  $r$ ).

By substituting in Eq. (4), we receive

$$Z = H \cdot X + \nu = \tilde{H}X + \begin{pmatrix} \nu_x \\ \nu_y \\ \nu_z \\ \nu_D - d\hat{x}u_x - d\hat{y}u_y - d\hat{z}u_z \end{pmatrix} = \tilde{H}X + \begin{pmatrix} \nu_x \\ \nu_y \\ \nu_z \\ \nu_D - d\hat{r}^\top \cdot u \end{pmatrix}$$

Since  $\tilde{H}$  is the observation model that the KF uses in practice, the effective observation noise is  $(\nu_x, \nu_y, \nu_z, \nu_D - d\hat{r}^\top \cdot u)^\top$ , whose covariance is

$$\tilde{R} = \begin{pmatrix} \sigma_x^2 & & & \\ & \sigma_y^2 & & \\ & & \sigma_z^2 & \\ & & & \sigma_D^2 + C \end{pmatrix} = R + \begin{pmatrix} 0 & & & \\ & 0 & & \\ & & 0 & \\ & & & C \end{pmatrix} \quad (5)$$

assuming that  $d\hat{r}^\top \cdot u \sim N(0, C)$  for some  $C > 0$ , and that both positional errors  $d\hat{x}, \nu_x$  are independent of the velocity  $u_x$  (the latter keeps the zero correlations, e.g.,  $\text{Corr}(d\hat{x} \cdot u_x, \nu_x) = E(d\hat{x} \cdot u_x \cdot \nu_x) = E(d\hat{x}\nu_x)E(u_x) = 0$ , and thus the diagonal  $\tilde{R}$ ).

Eq. (5) provides the theoretical explanation for Figure 4b in Section 3, where we see that the optimization of  $R$  increases the variance of the Doppler signal compared to the variance of the positional signal. Figure 4b also shows a decrease in the positional variance (not only an increase in Doppler’s variance), which is not explained by the analysis above. This is caused by the fact that when  $Q \equiv 0$ , the absolute values of  $R$  have quite minor importance compared to the relative values between the components – hence the optimization increases Doppler’s variance compared to positional variance, but is quite indifferent to their scale. Indeed, re-scaling of the optimized  $R$  provided indistinguishable empirical results.

Note that in this private case of Toy benchmark, the gap between estimation and optimization could be easily solved by modifying the estimation from  $R := \text{Cov}(\{z_t - H(x_t) \cdot x_t\})$  to  $R := \text{Cov}(\{z_t - H(z_t) \cdot x_t\})$ . However, this correction does not guarantee optimal results beyond the Toy benchmark, and in particular did not demonstrate significant improvement in the other benchmarks defined in Section 3. Indeed, while certain private cases can be modeled and solved analytically through effective noise estimation, optimization of the parameters provides a more robust solution.

## E Optimized Kalman Filter for Video Tracking

Radar tracking is an interesting domain with unique properties such as non-linear observation model and radial observation noise. In this domain, Section 3 demonstrates the sub-optimality of KF with estimated noise parameters, compared to a KF with optimized parameters. In this section, we compare the two in the popular and arguably-simpler domain of video tracking, using the MOT20 dataset [Dendorfer et al., 2020] (available under *Creative Commons Attribution-NonCommercial-ShareAlike 3.0* License).

MOT20 includes several videos with multiple targets (mostly pedestrians) to track. The dataset also includes the ground-truth location and size of the targets in every frame of the videos. We consider these ground-truth states as direct observations, i.e., we assume to have a detector with zero observation error (which in particular makes the observation model linear, in contrast to the radar tracking problem).

More specifically, we characterize a target using the state  $X = (x, y, w, h, vx, vy) \in \mathbb{R}^6$  (two-dimensional location, size and velocity), and an observation as  $Z = (x, y, w, h)$ . Note that  $x, y, w, h$  are provided in the dataset and we derive  $vx, vy$  from  $x, y$ . The observation model  $H$  is known as described above, and for the motion model  $F$  we assume constant velocity and constant target size, leading to:

$$H = \begin{pmatrix} 1, 0, 0, 0, 0, 0 \\ 0, 1, 0, 0, 0, 0 \\ 0, 0, 1, 0, 0, 0 \\ 0, 0, 0, 1, 0, 0 \end{pmatrix}, F = \begin{pmatrix} 1, 0, 0, 0, 1, 0 \\ 0, 1, 0, 0, 0, 1 \\ 0, 0, 1, 0, 0, 0 \\ 0, 0, 0, 1, 0, 0 \\ 0, 0, 0, 0, 1, 0 \\ 0, 0, 0, 0, 0, 1 \end{pmatrix}$$

$Q$  and  $R$  are estimated or optimized with relation to the train data, as described in Section 3. For the train data we use MOT20-01, MOT20-02, MOT20-03, and for the test data MOT20-05. In particular, our test data comes from an entirely different video than the train data, hence the testing is less prone to overfit. The goal function for the optimization is the MSE (mean square error) of the location  $x, y$  after the prediction step (note that in absence of observation noise, the error of the update step is simply zero).

As shown in Figure 3, the optimized model (OKF) reduces the prediction errors (MSE) by 18% in comparison to a KF with standard noise estimation. The significance level of the results is also indicated by the huge z-value  $z = 125$ , corresponding to the errors difference (calculated as  $z = \text{mean}(\Delta \text{err}) / \text{std}(\Delta \text{err}) \cdot \sqrt{N_{\text{samples}}}$ ). The results indicate that the sub-optimality of noise estimation – as well as the benefits of parameters optimization – are a cross-domain phenomenon and are not limited to radar tracking or to non-linear observation models.



Figure 7: A sample of 2 targets in the first frame of the test video in MOT20. The true trajectories of the targets are shown along with the predictions of KF and OKF (each prediction is done one time-step in advance).

## F Cholesky Gradient Optimization

Section 4 discusses an efficient method to apply gradient-based optimization to SPD matrices, based on parameterization of the SPD matrix using Cholesky decomposition [Pineiro and Bates, 1996]. This section presents this method more formally.

We consider an objective function  $f(x; A)$  to be minimized, where  $x$  is the input and  $A \in \mathbb{R}^{n \times n}$  are parameters formed as a SPD matrix. We define  $A(L) := LL^\top$  and

$$(L(\theta))_{ij} := \begin{cases} 0 & \text{if } i < j \\ e^{\theta_{n(n-1)/2+i}} & \text{if } i = j \\ \theta_{(i-2)(i-1)/2+j} & \text{if } i > j \end{cases}$$

where  $\theta \in \mathbb{R}^{n(n+1)/2}$ . We also denote the optimization update rule by  $u(\theta, g)$ , where  $\theta$  are the current parameters and  $g$  is the current gradient. For example, for the classic gradient descent,



$u(\theta, g) = \theta - \alpha g$ . Using these notations, the optimization method becomes as simple as Algorithm 1. This algorithm (with Adam’s update rule) was used for all the KF optimizations in this work.

---

**Algorithm 1:** Cholesky Gradient Optimization

---

**Input:** objective  $f$ ; update rule  $u$ ; data  $X$ ; initial parameters  $\theta_0 \in \mathbb{R}^{n(n+1)/2}$ ;

**Output:** SPD matrix  $A \in \mathbb{R}^{n \times n}$ ;

$\theta \leftarrow \theta_0$ ;

**for** training epoch **do**

**for** data sample  $x$  in  $X$  **do**

$g \leftarrow \nabla_{\theta} f(x; A(L(\theta)))$ ;

$\theta \leftarrow u(\theta, g)$ ;

Return  $A(L(\theta))$ ;

---

Note that the diagonal of  $L(\theta)$  could be replaced by any increasing positive transformation. In fact, we could even drop the positive transformation and allow non-positive diagonal entries in  $L$ : this would only eliminate the uniqueness of the parameterization, and would allow  $A$  to be positive *semi*-definite.

## G Detailed Results

Figures 8-12 below provide additional details about the experiments discussed in Sections 5,3.

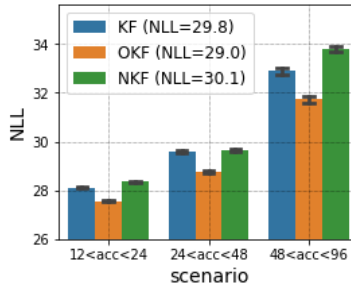
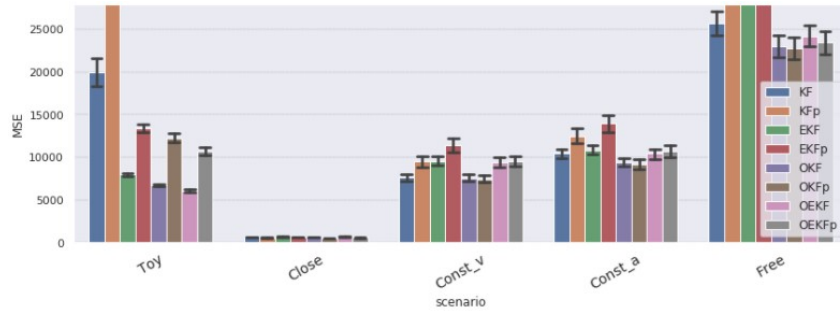
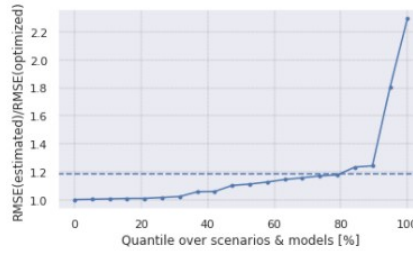


Figure 8: Negative-log-likelihood errors of different tracking models, over targets with different ranges of acceleration. This is analog to Figure 5a, but measures NLL rather than MSE.



(a)



(b)

Figure 9: (a) Errors of different tracking models over different benchmarks. This is a different visualization of the results of Table 1. Note that the optimized models (the last four) tend to yield better and more stable results than the estimated models. (b) The RMSE ratio between the estimated models and the optimized ones, over all the benchmarks and designs discussed in Section 3. Note that all the ratios are above 1, i.e., all the models in all the benchmarks had smaller errors when tuned by optimization. The horizontal line represents the average ratio.

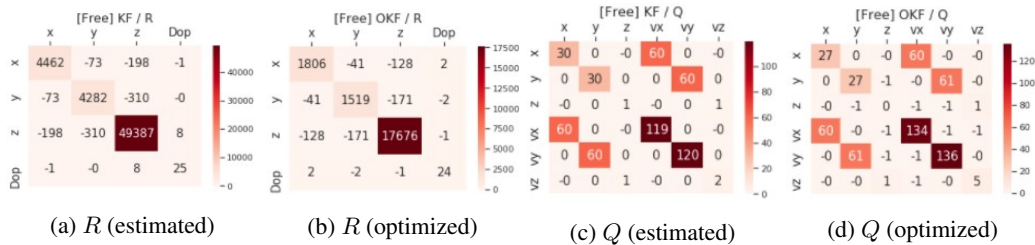
(a)  $R$  (estimated)(b)  $R$  (optimized)(c)  $Q$  (estimated)(d)  $Q$  (optimized)

Figure 10: The observation noise ( $R$ ) and prediction noise ( $Q$ ) matrices obtained in a (Cartesian) KF by noise estimation and by optimization with relation to  $MSE$  and  $NLL$ , based on the dataset of the Free-motion benchmark.

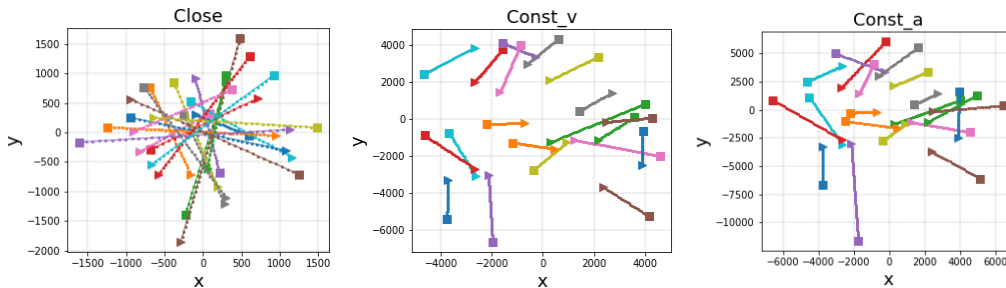


Figure 11: Samples of targets trajectories in the various benchmarks described in Section 3, projected onto the horizontal plane. This is an extension of Figures 2b,2c for the rest of the benchmarks.

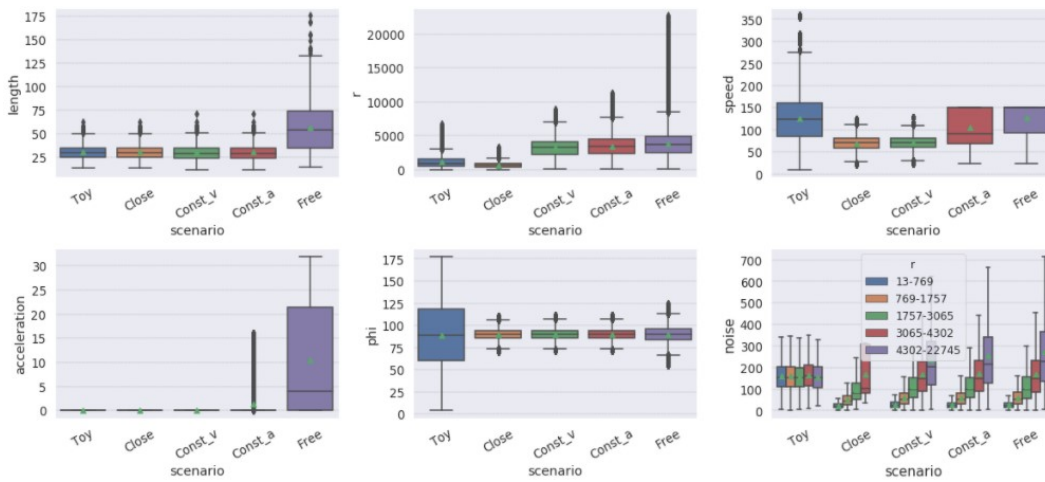


Figure 12: Descriptive statistics of the various benchmarks of Section 3: duration of targets trajectories; distance from the radar; targets speed; targets acceleration; motion direction (90 degrees correspond to horizontal motion); and observation errors vs. distance from radar.